Electronic Supplementary Material (ESI) for Journal of Materials Chemistry A.
This journal is © The Royal Society of Chemistry 2015

Supporting Information

Magnetically Driven Bi_2O_3/BiOCl-Based Hybrid Microrobots for Photocatalytic Water Remediation

Fajer Mushtaq,[a,g] Miguel Guerrero,[b,g] Mahmut Selman Sakar,[a] Marcus Hoop,[a] André M. Lindo,[a] Jordi Sort,[c] Xiangzhong Chen,[a] Bradley J. Nelson,[a] Eva Pellicer[b] and Salvador Pané[a,*]

(a)

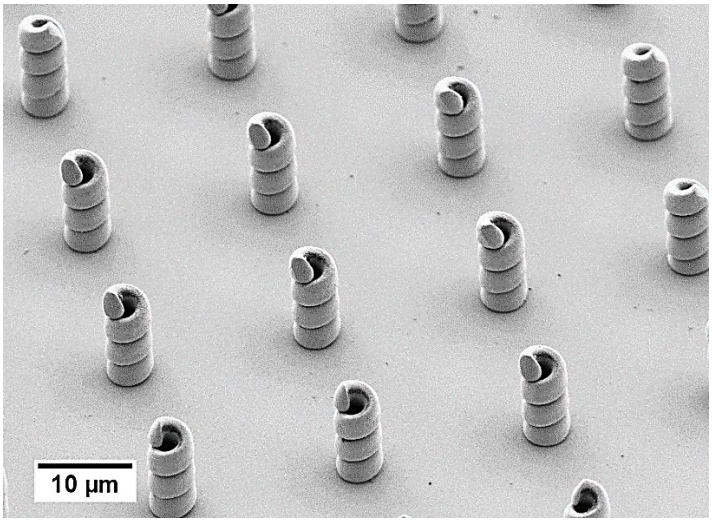

(b)

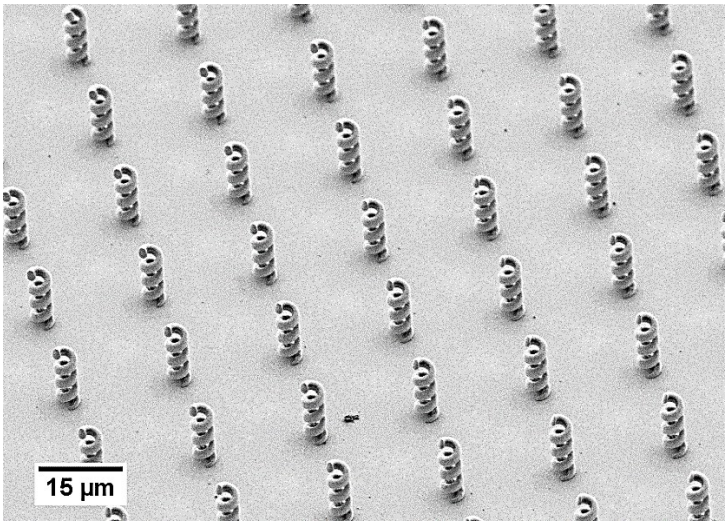

(c)

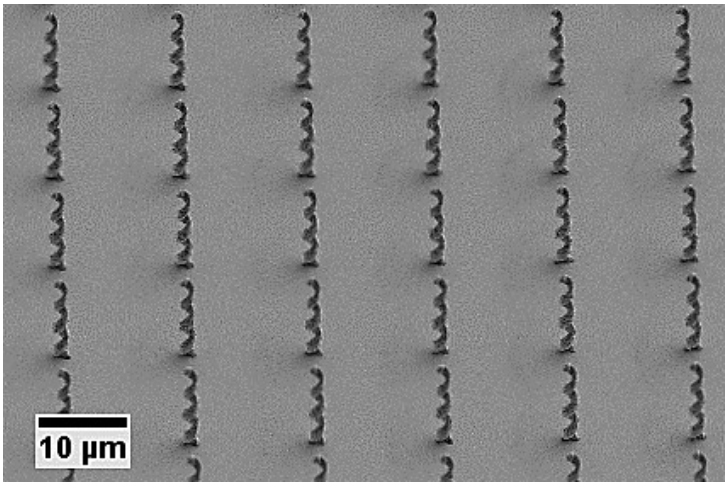

Fig. S1 SEM images of CoNi helical structures made using 3D photolithography. Figures (a-c) show a few examples of the versatile shapes that can be easily tuned and fabricated using 3D photolithography.

(a)

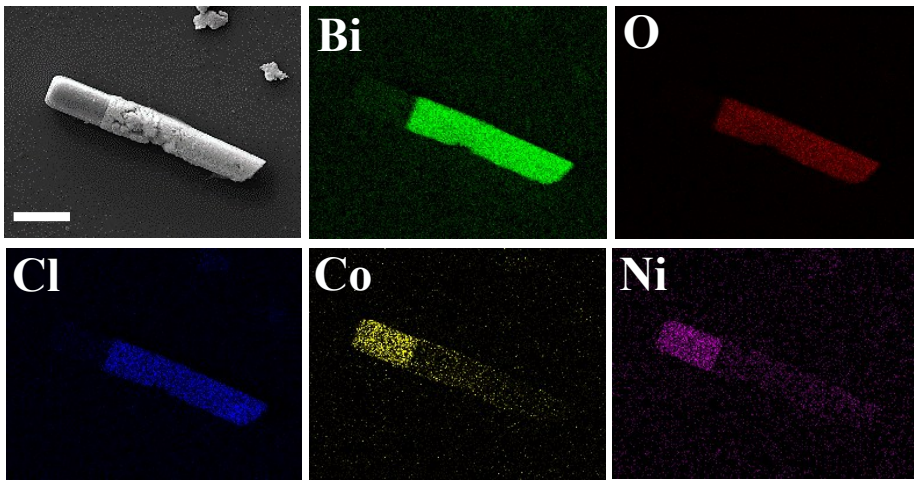

(b)

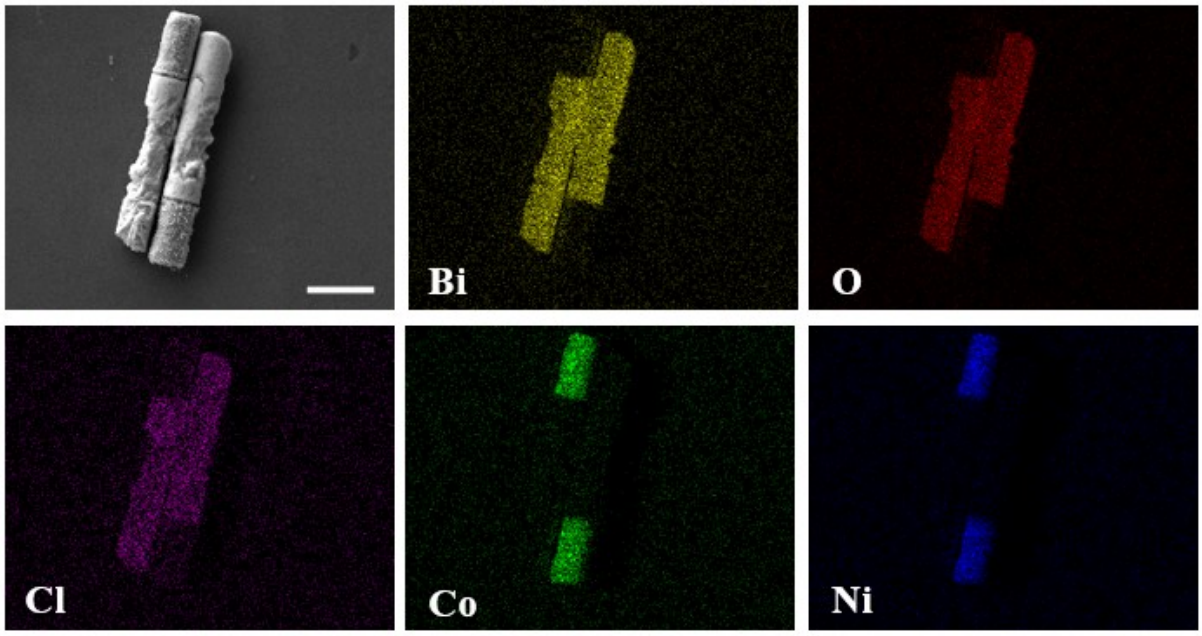

(c)

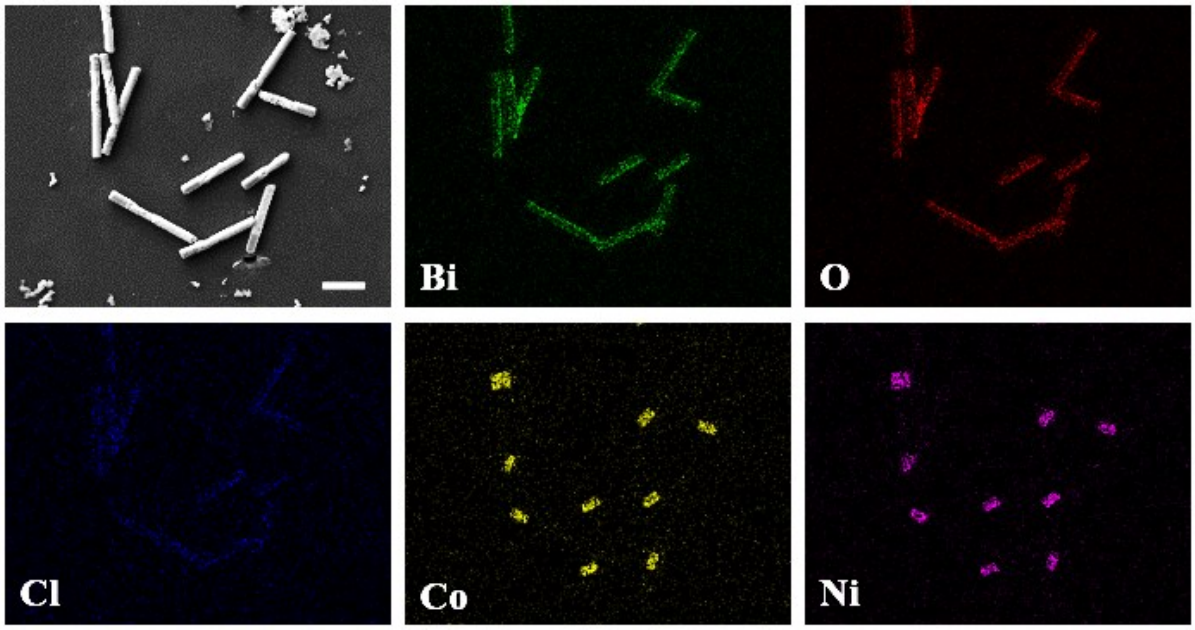

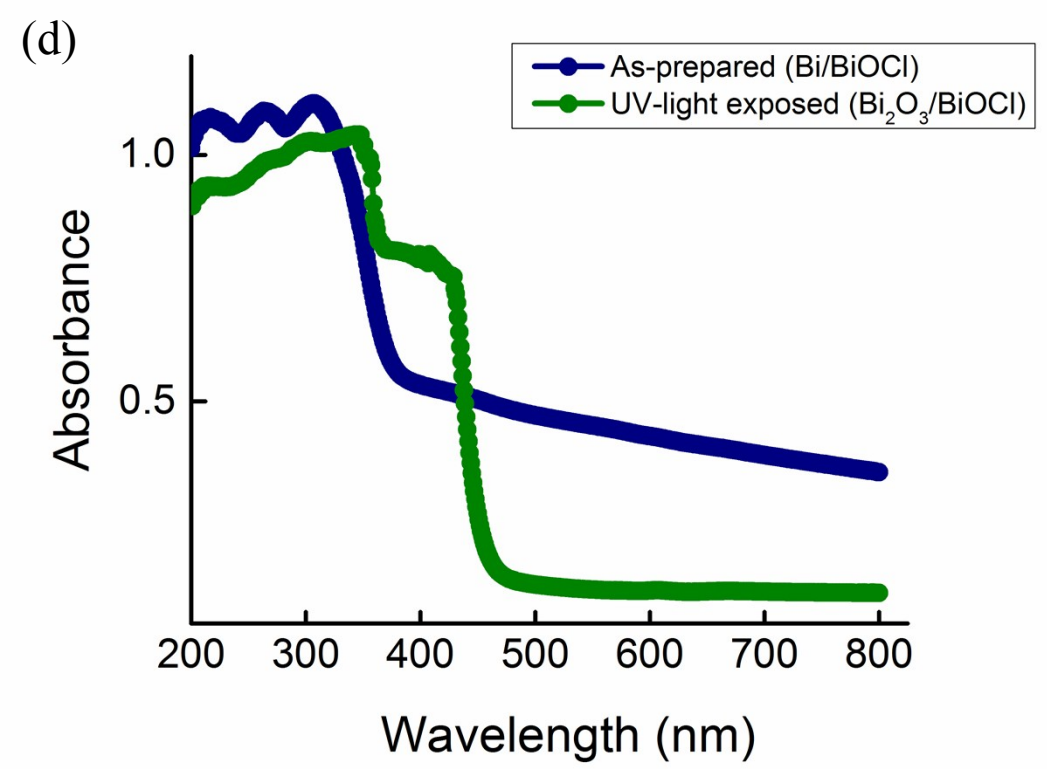

Fig. S2 (a) EDX map performed on an as-prepared hybrid micropillar. The map shows a uniform distribution of the different elements present in the hybrid micropillar. Scale bar 2 μm, (b) EDX map performed on two UV-light exposed hybrid micropillars. In comparison to the EDX map presented for the as-prepared hybrid structure in (a), a higher intensity is observed for oxygen signal while Bi map shows a slightly lower intensity, (c) EDX map performed on a few UV-light exposed hybrid micropillars showing uniform distribution of elements for all the structures, (d) UV-vis diffuse reflectance spectroscopy performed on as-prepared and UV-light exposed samples show a clear visible light spectrum activation when Bi/BiOCl was converted to Bi_2O_3/BiOCl after exposure to UV-light. Scale bars: 2 μm, 2 μm and 3 μm.

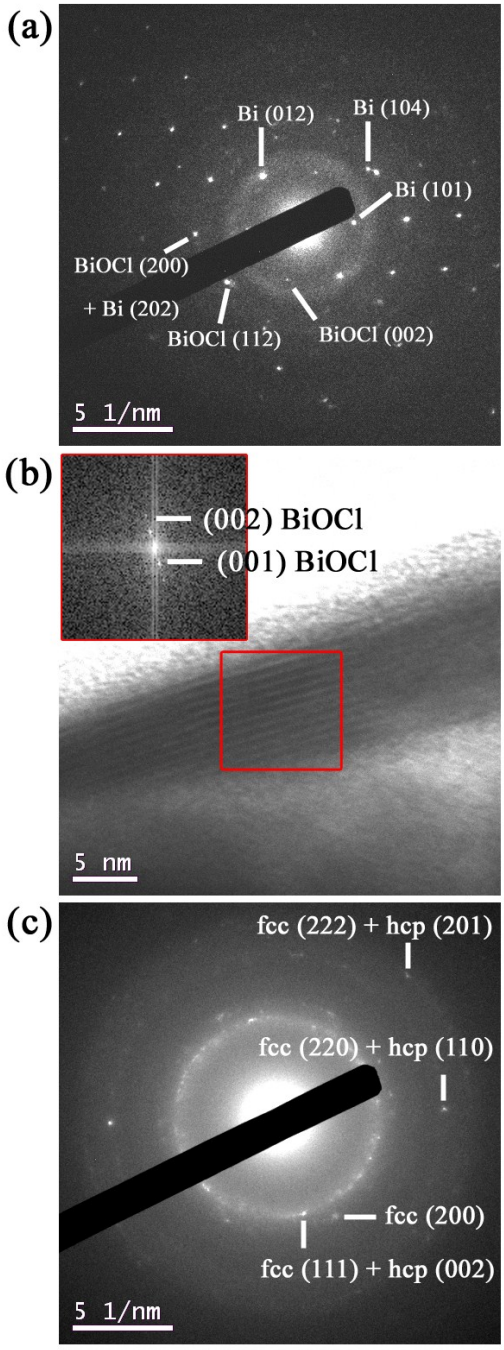

Fig. S3 (a) Selected area electron diffraction (SAED) pattern and (b) high resolution TEM image taken on a piece of Bi/BiOCl segment. The spots in (a) match either Bi or BiOCl phases. The inset in (b) is the fast fourier transform (FFT) of the area enclosed in the red square. (c) SAED pattern taken on a piece of CoNi segment. The rings show the existence of both hexagonal-close packed (hcp) and face-centered cubic (fcc) CoNi phases. The preparation of the sample was as follows: the ITO substrate was gently scratched off to gather small pieces from the micropillars. The collected pieces were suspended in ethanol and subjected to ultrasonication in order to break them in smaller pieces. A couple of drops of the resulting suspension were subsequently dropwise added to carbon-coated Cu TEM grids. In spite of the sonication step, the fragments were still rather thick so imaging had to be performed at the edge.

(a)

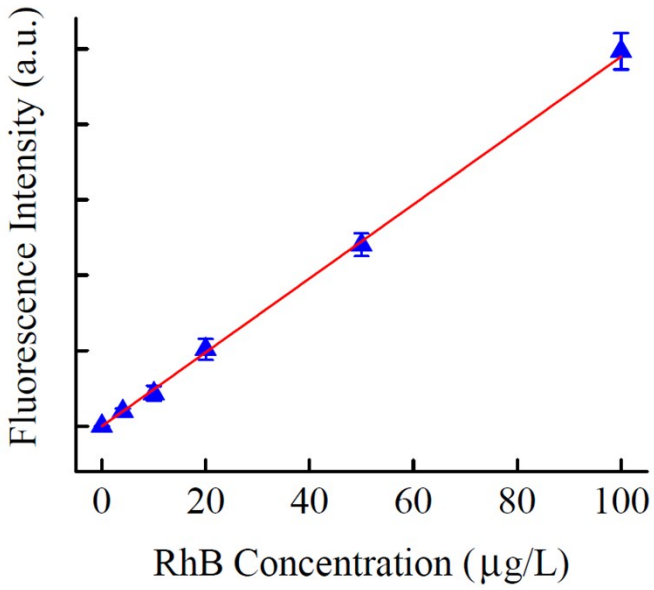
Fluorescence Intensity (a.u.)
0
20
40
60
80
100
RhB Concentration (μg/L)

(b)

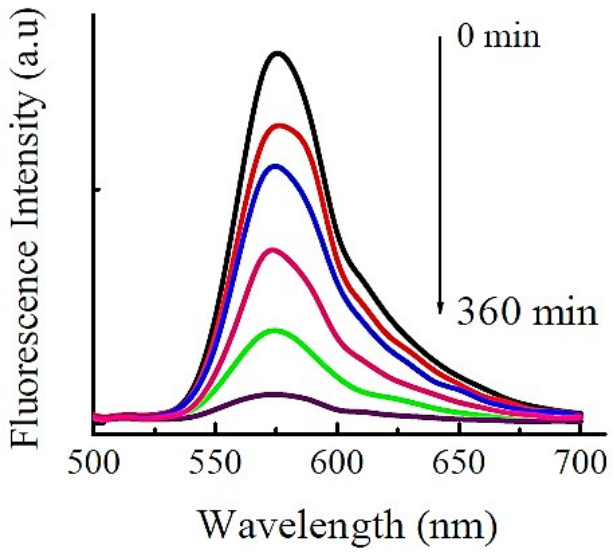
Fluorescence Intensity (a.u)
0 min
360 min
500
550
600
650
700
Wavelength (nm)

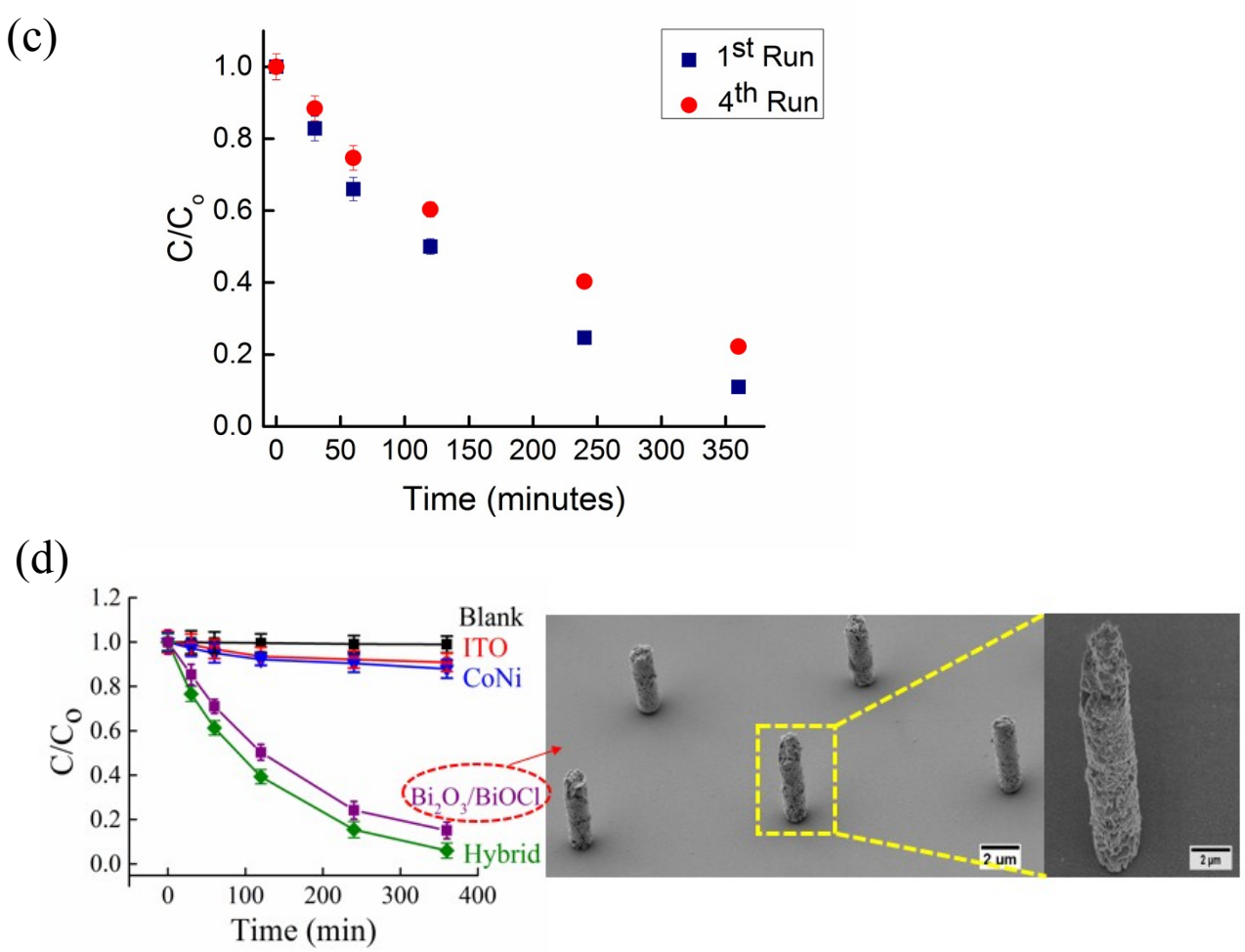

Fig. S4 Photocatalytic degradation plots of hybrid micropillars. (a) calibration curve used for selecting a RhB concentration in the linear range; (b) shows a gradual decrease in the fluorescence intensity of RhB over time in the presence of hybrid micropillars, indicating a decrease in RhB dye concentration due to its photocatalytic degradation (c) RhB degradation plot obtained for substrate-released hybrid pillars which were collected for reuse using a permanent magnet, (d) photocatalytic degradation plots of RhB showing that for the hybrid structures the degradation rate is slightly faster than for only Bi_2O_3/BiOCl micropillars. Both structures however show a similar degradation trend.

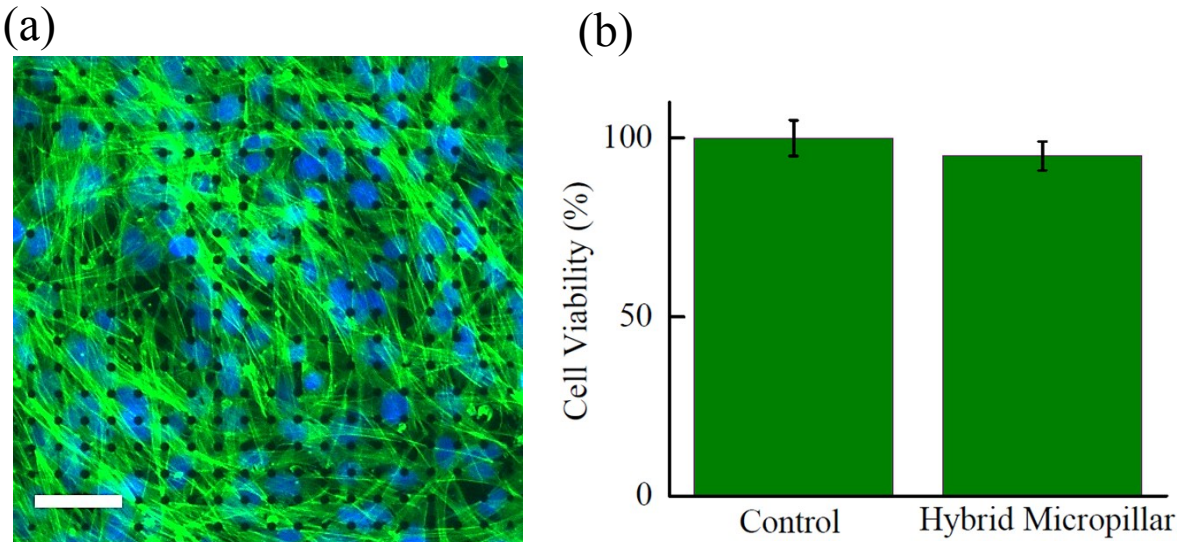

Fig. S5 Cytotoxic study on hybrid micropillars. (a) fluorescence image of NIH 3T3 fibroblast cells cultured on an array of free-standing hybrid pillars with stained nucleus (blue) and actin (green) show healthy cells with extending actin fibers; (b) MTT Cytotoxicity study shows that the sample with free-standing hybrid micropillar has a 95% cell viability in comparison to the control sample. Scale bar shown is 40 µm.

Videos demonstrating magnetic manipulation

Video S1: A hybrid micropillar showing a surface walker motion at 2 Hz at 2x.

Video S2: A hybrid microhelix showing a corkscrew motion at 2 Hz.